

Structure of a Superhydrophilic Surface: Wet Chemically Prepared Rutile-TiO₂(110)(1 × 1)

J. P. W. Treacy,[†] H. Hussain,^{†,‡} X. Torrelles,[§] G. Cabailh,^{||} O. Bikondoa,[⊥] C. Nicklin,[#]
G. Thornton,[▽] and R. Lindsay^{*,†,‡}

[†]Corrosion and Protection Centre, School of Materials, The University of Manchester, Sackville Street, Manchester M13 9PL, United Kingdom

[‡]Photon Science Institute, The University of Manchester, Manchester M13 9PL, United Kingdom

[§]Institut de Ciència de Materials de Barcelona (CSIC), Campus UAB, 08193 Bellaterra, Spain

^{||}Sorbonne Université, UMR CNRS 7588, Institut des NanoSciences de Paris, 4 Place Jussieu, 75252 Paris Cedex 05, France

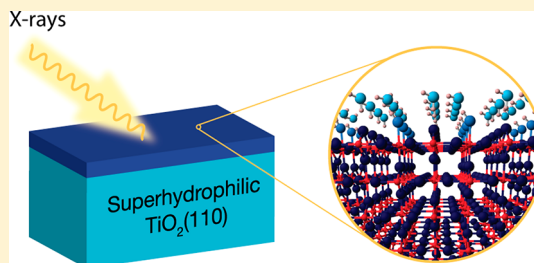
[⊥]Department of Physics, University of Warwick, Gibbet Hill Road, Coventry CV4 7AL, United Kingdom

[#]Diamond Light Source Ltd., Diamond House, Harwell Science and Innovation Campus, Didcot, Oxfordshire OX11 0DE, United Kingdom

[▽]London Centre for Nanotechnology and Chemistry Department, University College London, 20 Gordon Street, London WC1H 0AJ, United Kingdom

Supporting Information

ABSTRACT: Surface X-ray diffraction has been employed to quantitatively determine the geometric structure of an X-ray-induced superhydrophilic rutile-TiO₂(110)(1 × 1) surface. A scatterer, assumed to be oxygen, is found at a distance of 1.90 ± 0.02 Å above the five-fold-coordinated surface Ti atom, indicating surface hydroxylation. Two more oxygen atoms, situated further from the substrate, are also included to achieve the optimal agreement between experimental and simulated diffraction data. It is concluded that these latter scatterers are from water molecules, surface-localized through hydrogen bonding. Comparing this interfacial structure with previous studies suggests that the superhydrophilicity of titania is most likely to be a result of the depletion of surface carbon contamination coupled to extensive surface hydroxylation.



INTRODUCTION

Ever since Wang et al.'s discovery that UV irradiation of titania results in a superhydrophilic surface,¹ there has been a great deal of effort to both exploit and understand this novel phenomenon. Significant success has been achieved in the former of these two goals, with applications including self-cleaning windows and antifogging mirrors.^{2–5} In contrast, uncertainty still remains as to the origin of the superhydrophilicity. Currently, there are a number of potential explanations to be found in the literature,^{1,3,6–10} but none are supported by compelling experimental evidence. For example, it is proposed that the superhydrophilicity is simply a result of the removal of surface carbon contamination.⁶ Other researchers suggest that modification of the surface structure/chemistry of the titania substrate (e.g., surface hydroxylation) underpins this macroscopic property.⁹ Longer range structural changes are also purported to be important, including the formation of nanoscale hydrophobic and hydrophilic domains.^{1,11,12} Here we directly address this topic, employing surface X-ray diffraction (SXRD) to quantitatively determine the structure of a model titania

surface, rutile-TiO₂(110), that exhibits superhydrophilicity induced through X-ray exposure.

Previously, Shirasawa et al. (SEL) have undertaken SXRD measurements from rutile-TiO₂(110) to identify changes in surface structure associated with the UV-induced hydrophobic-to-hydrophilic transition.¹³ They report that the application of a wet chemical preparation (WCP) recipe to the substrate resulted in a hydrophobic (1 × 1) surface termination, which became hydrophilic upon UV irradiation. It is suggested that this transition is associated with the presence of surface hydroxyls (OH), as surface five-fold-coordinated titanium atoms (Ti_{5c}) and bridging oxygens (O_b) become hydroxylated following the exposure to UV light. Figure 1 illustrates the changes in interface geometry concluded in ref 13.

In this Article, we revisit the structure of the superhydrophilic rutile-TiO₂(110)(1 × 1) surface. A WCP method

Special Issue: Hans-Joachim Freund and Joachim Sauer Festschrift

Received: January 9, 2019

Revised: February 6, 2019

Published: February 6, 2019

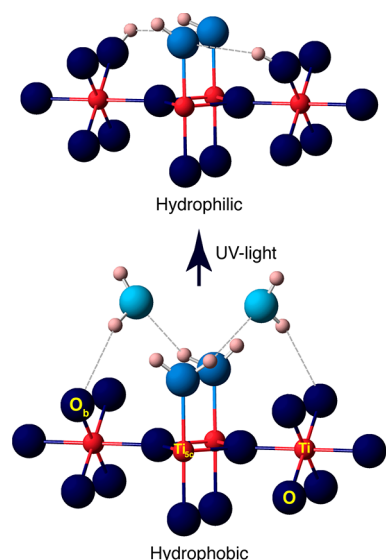


Figure 1. Ball-and-stick models showing the UV-induced (hydrophobic to hydrophilic) changes in interface geometry for rutile-TiO₂(110), as concluded by SEL from SXRD data.¹³ Red spheres are Ti atoms and darker (lighter) blue spheres are substrate (adsorbate) oxygen atoms. H atoms (pink spheres) are depicted, although they were not explicitly included in SEL's structure determination. Possible hydrogen bonds are indicated by dashed lines.

is again employed for sample preparation, but with X-rays being used to induce superhydrophilicity. Similar to ref 13, the surface is found to be extensively hydroxylated, including OH bound to Ti_{5c}. The diffraction data acquired in this study, however, resemble much more closely those acquired from the hydrophobic termination in ref 13. As argued in detail below, this somewhat unexpected finding suggests that the analysis and interpretation of SEL¹³ require revision.

EXPERIMENTAL METHODS

Concerning sample preparation, a previously published WCP recipe¹⁴ was applied to the rutile-TiO₂(110) substrate (10 × 10 × 1 mm sample from PI-KEM), which is known to produce a well-ordered (1 × 1) surface termination. In brief, this procedure involves sequential sonication in acetone, ethanol, and deionized water and then annealing in air at ~973 K for ~90 min. Subsequently, the sample is immersed in aqua regia solution (3:1 by volume ratio of concentrated HCl and HNO₃) at room temperature for ~45 min. The final UV-ozone treatment step described in ref 14 was not undertaken in this study. Please note that the TiO₂ sample remained transparent following the application of this WCP recipe, indicating that there was no bulk reduction.¹⁵

Upon the completion of surface preparation, surface hydrophilicity was evaluated by delivering a small droplet of deionized water to the TiO₂(110) surface using a syringe/hypodermic needle. Once the contact angle of the deposited droplet had been determined by visual inspection, the sample was blown dry with high-purity nitrogen. The sample was then transferred to the diffractometer located in EH1 of beamline I07 at the Diamond Light Source synchrotron facility for SXRD measurements. It was mounted in an X-ray transparent (cylindrical Kapton window) environmental cell. Once the cell was closed up, high-purity helium was flowed through it for the duration of the SXRD measurements. It should be noted that it

was not possible to monitor either oxygen or water vapor concentration within the cell.

SXRD data were collected at an incidence angle of 1° with the substrate at room temperature using a photon energy of $h\nu = 17.7$ keV and a 2D Pilatus photon detector. A systematic series of X-ray reflections was acquired from the sample; that is, for a given (h, k) integer, data were measured as a function of l to facilitate the generation of so-called crystal truncation rods (CTRs). h , k , and l are the reciprocal lattice vectors. They are defined with reference to the real-space (1 × 1) unit cell of the (110) surface, described by lattice vectors ($\mathbf{a}_1, \mathbf{a}_2, \mathbf{a}_3$) which are parallel to the $[\bar{1}10]$, $[001]$, and $[110]$ directions, respectively; $a_1 = a_3 = a\sqrt{2}$, and $a_2 = c$, where $a = 4.593$ Å and $c = 2.958$ Å are the lattice constants of the tetragonal rutile crystal structure. A surface-sensitive reflection (i.e., one that is located well away from any bulk Bragg peak), namely, $(-1, 0, 0.9)$, was recorded at regular intervals to monitor the surface integrity.

To facilitate fully quantitative structure determination, the raw 2D diffraction images were integrated, including background removal, and corrected¹⁶ to enable plots of structure factor versus perpendicular momentum transfer for each CTR to be compiled. This procedure generated a total of 1068 nonequivalent reflections from eight distinct CTRs. The ROD software¹⁷ was employed to simulate these data, with structural (and nonstructural) parameters being refined to achieve the overall best fit between experiment and theory. Reduced χ^2 was used to evaluate the goodness of fit, which is defined as follows¹⁸

$$\chi^2 = \frac{1}{N - P} \sum_{i=1}^N \left(\frac{|F_i^{\text{exp}}(hkl)| - |F_i^{\text{th}}(hkl)|}{\sigma_i^{\text{exp}}(hkl)} \right)^2$$

N is the number of measured structure factors, P is the number of parameters optimized during fitting, and $F_i^{\text{exp}}(hkl)$ and $F_i^{\text{th}}(hkl)$ are the experimental and theoretically calculated structure factors, respectively. $\sigma_i^{\text{exp}}(hkl)$ is the uncertainty associated with $F_i^{\text{exp}}(hkl)$. χ^2 behaves such that a value of 1 indicates that experiment and theory are essentially coincident, with agreement decreasing with increasing χ^2 . The quoted precision of each fitted parameter is determined by systematically varying the parameter about its optimal value and for each step optimizing all other parameters, until χ^2 has increased by $1/(N - P)$ from its minimum value.¹⁸

RESULTS AND DISCUSSION

The application of our WCP recipe to the rutile-TiO₂(110) sample resulted in a deionized water contact angle of ~80°. This value is consistent with that reported in ref 14 for a (1 × 1) surface termination subsequent to immersion in aqua regia but not exposed to UV-ozone treatment. Following exposure to I07's photon beam, the contact angle was found to fall to essentially 0°; that is, a superhydrophilic transition was induced by X-ray exposure. All diffraction measurements were undertaken with the rutile-TiO₂(110)(1 × 1) surface in this state; a contact-angle measurement at the end of data collection indicated that a value of 0° was maintained throughout this period. Data from the $(-1, 0, 0.9)$ reference reflection also revealed no substantive surface degradation.

Figure 2 shows four of the experimental CTRs acquired in the current study (black markers with error bars), together with equivalent data collected by SEL¹³ from rutile-TiO₂(110) following UV exposure (blue markers with error bars). A priori, as both data sets were recorded from superhydrophilic

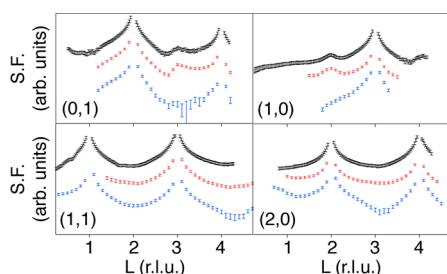


Figure 2. Comparison of the (0, 1, *l*), (1, 0, *l*), (1, 1, *l*), and (2, 0, *l*) experimental CTRs acquired from X-ray-induced superhydrophilic rutile-TiO₂(110) in the current study with data from SEL.¹³ Current study: black markers with error bars; pre-UV exposure from SEL:¹³ red markers with error bars; post-UV exposure from SEL:¹³ blue markers with error bars. Profiles are systematically offset for clarity.

surfaces, it was expected that they would be very similar. However, there are significant differences. For example, the local maxima in our data at (0, 1, ~3) and (1, 0, ~2), are not replicated in those from SEL. In contrast, our CTR profiles are much more comparable to those reported by SEL for their pre-UV exposure (hydrophobic) surface. These data are also shown in Figure 2 as red markers with error bars. We note that on an adsorbate-free rutile-TiO₂(110)(1 × 1) surface, prepared in ultrahigh vacuum (UHV), the aforementioned local maxima are associated with significant displacements of surface atoms away from their bulk positions;¹⁹ that is, they are not a direct signature of surface hydrophilicity. An absence of such features may be a result of either a more bulk-like termination or surface roughening.

Considering the qualitative comparison outlined above, it was expected that fitting of our experimental SXR data would result in the hydrophobic structure determined by SEL,¹³ where molecular H₂O is bound atop Ti_{sc} (see Figure 1). Figure 3 shows the best fit (blue line) achieved using SEL's hydrophobic structure as a starting point and simply allowing the displacement of both atomic positions and nonstructural parameter values. As indicated by $\chi^2 = 2.60$, as well as visual inspection, the experiment–theory agreement is far from

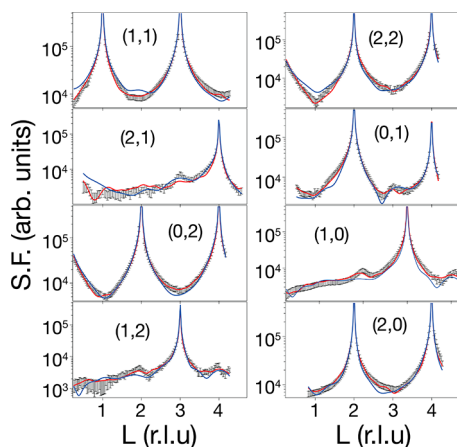


Figure 3. Comparison of experimental CTR data (black markers with error bars), acquired from X-ray-induced superhydrophilic rutile-TiO₂(110), and theoretical best-fit simulations. Solid blue line indicates the best fit achieved following relaxation of the hydrophobic structure reported by SEL.¹³ Solid red line indicates the overall best fit, with $\beta = 0.24$ and a surface fraction of 0.96.

perfect, suggesting that the correct structural solution had not been found. On this basis, we explored other potential surface terminations, including those consistent with the presence of surface hydroxyls. The resulting overall best fit to the experimental CTRs is shown in Figure 3 (red line). To achieve this fit, 78 parameters were optimized, that is, 51 atomic coordinates, 21 Debye–Waller (DW) factors, a scale factor, surface roughness (β), three fractional occupancies, and surface fraction. The corresponding χ^2 is 1.05; that is, there is an excellent level of agreement between the experimental and simulated data.

The optimum geometry of the first few atomic layers emerging from the best fit to the experimental CTR profiles is depicted in Figure 4. Selected corresponding interatomic

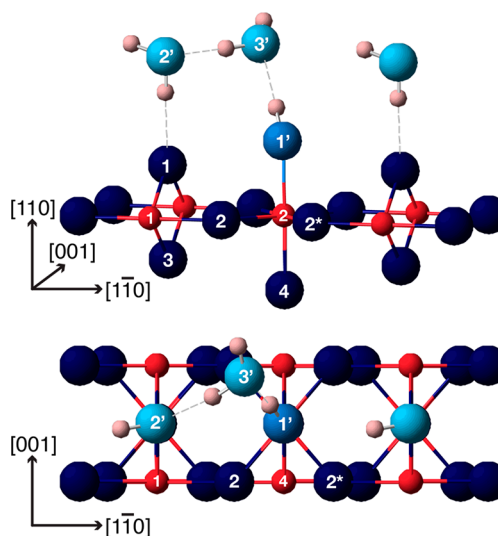


Figure 4. Ball-and-stick models of the X-ray-induced superhydrophilic rutile-TiO₂(110) surface structure determined from SXR data. Perspective (top) and plane (bottom) views are shown. Red spheres are Ti atoms, and darker (lighter) blue spheres are substrate (adsorbate) oxygen atoms. H atoms (pink spheres) are depicted, although they were not explicitly included in the structure determination. Possible hydrogen bonds are indicated by dashed lines. The numerical labeling of the atoms is employed in Table 1 and Table S1 for identification purposes. Symmetry-paired atoms are denoted by *.

distances are listed in Table 1. A ball-and-stick model showing all atoms displaced during fitting is shown in Figure S1, along with a complete list of the optimized coordinates, DW factors,

Table 1. Selected Interatomic Distances Derived from Atomic Coordinates (Table S1) of Optimized Superhydrophilic TiO₂(110)(1 × 1) Structure

atoms	interatomic distance (Å)
O(3')–O(2')	2.70 ± 0.06
O(3')–O(1')	2.65 ± 0.05
O(2')–O(1)	2.68 ± 0.03
O(1')–Ti(2)	1.90 ± 0.02
O(1)–Ti(1)	1.83 ± 0.02
O(2)–Ti(1)	1.98 ± 0.02
O(2)–Ti(2)	1.95 ± 0.02
O(3)–Ti(1)	1.94 ± 0.01
O(4)–Ti(2)	1.94 ± 0.01

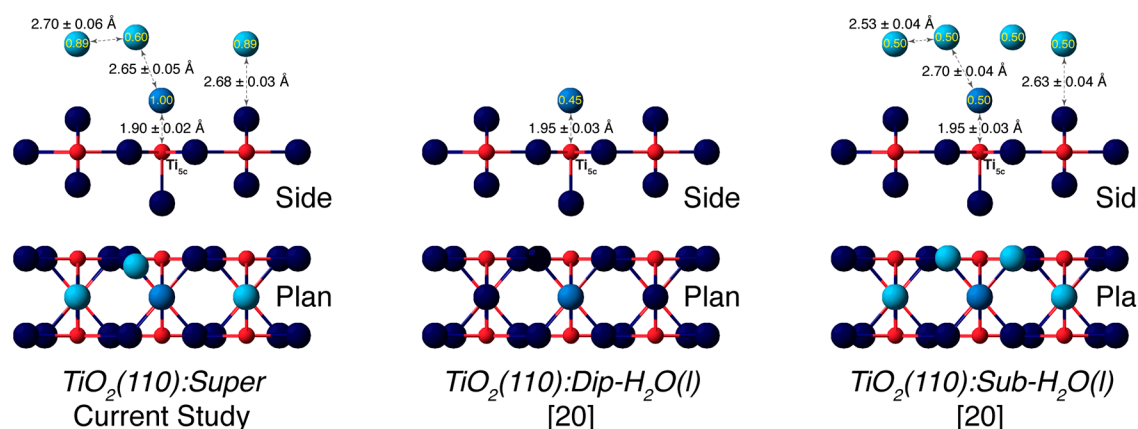


Figure 5. Ball-and-stick models of the optimum interfacial structures determined from SXR D for X-ray-induced superhydrophilic rutile- $\text{TiO}_2(110)$ (current study), rutile- $\text{TiO}_2(110)$ subsequent to dipping in $\text{H}_2\text{O}(l)$,²⁰ and rutile- $\text{TiO}_2(110)$ submerged in $\text{H}_2\text{O}(l)$.²⁰ Side (top) and plane (bottom) views are shown. Red spheres are Ti atoms, and darker (lighter) blue spheres are substrate (adsorbate) oxygen atoms. Selected interatomic distances are annotated. Fractional occupancies of adsorbate oxygen atoms are indicated by the values inscribed on the lighter blue spheres.

and fractional occupancies in Table S1. Neglecting the details of atomic relaxation, the surface mimics the stoichiometry and geometry of bulk-terminated rutile- $\text{TiO}_2(110)(1 \times 1)$ but is decorated with oxygen species. Focusing on Ti_{5c} (labeled Ti(2)), an adsorbed oxygen atom (labeled O(1')) is located atop at a distance of $1.90 \pm 0.02 \text{ \AA}$, which is consistent with the presence of a bound terminal hydroxyl (OH_t).^{20,21} The experimental distance from ref 20 is $1.95 \pm 0.03 \text{ \AA}$, with a moderately longer distance of 2.07 \AA being obtained from molecular dynamics calculations.²⁰ Two additional non-substrate oxygen atoms (labeled O(2') and O(3')) are at somewhat greater distances from the topmost substrate atoms. O(2') is $2.68 \pm 0.03 \text{ \AA}$ above the bridging oxygen atom (labeled O(1)), with O(3')'s nearest neighbor being O(1') at a distance of $2.65 \pm 0.05 \text{ \AA}$. These interatomic separations suggest that oxygen atoms O(2') and O(3') arise from water molecules, which are localized through hydrogen bonding.²² For illustrative purposes, we have included H atoms in Figure 4 but stress that these species were not explicitly included during the generation of simulated SXR D data due to their negligible X-ray scattering.

Given the optimized structure displayed in Figure 4, it is interesting to compare this result with other pertinent studies. Focusing initially on SEL's work,¹³ the present diffraction data are very similar to those acquired from their hydrophobic surface, as demonstrated in Figure 2. Because our surface is superhydrophilic, as a result of X-ray exposure, this agreement presents a conundrum. One plausible explanation, arising from discussion with SEL,¹³ is that the $\sim 1 \text{ mm}^2$ footprint of the X-ray beam employed for their SXR D measurements induced superhydrophilicity only in this region. Hence the water contact-angle measurement, where the droplet employed covered a much larger surface area, did not reveal this local X-ray-induced superhydrophilicity. It should be noted that on I07 almost the entire sample surface would have been exposed to the X-ray beam during alignment and measurement.

On the basis that SEL's pre-UV-exposure surface is superhydrophilic in the area probed by the X-ray beam, then one further issue requires resolution. Specifically, despite the similar experimental data, the discrepancy between our optimized structure and SEL's needs to be understood, for example, the variation in the Ti(2)–O(1') distance ($1.90 \pm$

0.02 versus $2.09 \pm 0.03 \text{ \AA}$ ¹³). To this end, our experimental data set (eight CTRs) was reduced to match that of SEL (six CTRs), and fitting was undertaken. Under these conditions, we were able to effectively model the data with SEL's hydrophobic structure. On this basis, it is evident that fewer experimental CTRs leads to a local χ^2 minimum, resulting in a significantly different surface structure.

One other matter emerging from the preceding discussion is the origin of the UV-induced change in CTR profiles observed by SEL.¹³ Assuming that their pre-UV data is acquired from a superhydrophilic area of the rutile- $\text{TiO}_2(110)$ surface, then the observed changes cannot be accounted for by a hydrophobic–hydrophilic transition. This deduction implies that UV-irradiation leads to additional interfacial modification; that is, a unique surface structure is formed upon exposure to UV light. Currently, this suggestion is essentially conjecture, but is worthy of further investigation.

Having reconciled the results of this study with those of SEL,¹³ a comparison of the geometry of the current superhydrophilic termination with those reported for interfaces formed by the exposure of UHV-prepared $\text{TiO}_2(110)(1 \times 1)$ to liquid water ($\text{H}_2\text{O}(l)$) is worthwhile.²⁰ Figure 5 compares the current optimum structure ($\text{TiO}_2(110)$:Super) to that elucidated with SXR D following dipping of $\text{TiO}_2(110)(1 \times 1)$ into $\text{H}_2\text{O}(l)$ and measuring ex situ in UHV ($\text{TiO}_2(110)$:Dip- $\text{H}_2\text{O}(l)$) as well as that determined for $\text{TiO}_2(110)$ submerged in $\text{H}_2\text{O}(l)$ ($\text{TiO}_2(110)$:Sub- $\text{H}_2\text{O}(l)$). These three structures are similar but not identical. For example, both $\text{TiO}_2(110)$:Super and $\text{TiO}_2(110)$:Sub- $\text{H}_2\text{O}(l)$ exhibit oxygen atoms consistent with hydrogen-bonded H_2O molecules, although their configuration differs; such scatterers are not evident in the $\text{TiO}_2(110)$:Dip- $\text{H}_2\text{O}(l)$ data due to the acquisition in UHV. Turning to Ti_{5c} for each structure displayed in Figure 5, the distance to the atop oxygen atom is consistent with hydroxylation ($\text{Ti}_{5c}\text{--OH}_t$). However, $\text{TiO}_2(110)$:Super displays a slightly shorter $\text{Ti}_{5c}\text{--OH}_t$ distance ($1.90 \pm 0.02 \text{ \AA}$) than either $\text{TiO}_2(110)$:Dip- $\text{H}_2\text{O}(l)$ or $\text{TiO}_2(110)$:Sub- $\text{H}_2\text{O}(l)$ ($1.95 \pm 0.03 \text{ \AA}$). This variation may be a result of the former substrate being essentially fully oxidized, whereas the latter two were somewhat reduced as a result of substrate preparation in UHV.

Regarding the origin of the X-ray-induced superhydrophilicity of titania, the current SXRD data rule out the coexistence of hydrophilic and hydrophobic domains, as analysis indicates that almost the entire surface adopts the same geometry; that is, surface fraction is 0.96. It should be emphasized that the present study cannot be used to definitively rule out the existence of such domains on UV-exposed titania. Furthermore, because the diffraction data from $TiO_2(110):Dip-H_2O(l)$ were acquired in UHV from a surface not irradiated with either UV or X-rays during dipping, the mere presence of OH_t cannot be directly related to photoinduced superhydrophilicity. Given this result, one could suggest that the simple removal of surface carbon most likely underpins this property.⁶ It is, however, notable that the fractional occupancy of OH_t ($O(1')$) for $TiO_2(110):Super$ is approximately double that for either $TiO_2(110):Dip-H_2O(l)$ or $TiO_2(110):Sub-H_2O(l)$, that is, 1.00 compared to 0.45 and 0.50, respectively, as indicated in Figure 5. Hence, increased surface hydroxylation may play a role in TiO_2 superhydrophilicity, coupled to the loss of surface carbon. We remark that in ref 20 *ab initio* modeling suggests that the presence of OH_t is a result of (near) surface defects driving surface H_2O dissociation. Because the substrate in the current study is not expected to possess any significant concentration of defects, the hydroxyl species must arise from elsewhere. Almost certainly, it is photon-induced (or photo-excited electron) chemistry that produces these OH_t adsorbates, which may be the reason that a higher coverage is achieved; we note that this increase in surface hydroxylation is not simply related to carbon removal, as the surfaces in ref 20 are reported to be relatively carbon-free (≤ 0.1 monolayer).

Finally, we would like to comment on a recent elegant study suggesting that air- or aqueous-solution-exposed rutile- $TiO_2(110)$ is commonly decorated by carboxylate species.²³ On the basis that SXRD is not a spectroscopic probe, there is always the potential for misidentification of adsorbates, especially those exhibiting similar X-ray scattering characteristics (e.g., C and O). For the current study, however, we argue that this is not the case. Supporting evidence is two-fold. First, Auger spectra acquired from a superhydrophilic rutile- $TiO_2(110)$ surface, prepared following our WCP recipe, show no discernible carbon signal.¹⁴ Second, SXRD data were acquired from a superhydrophilic surface, which is inconsistent with the presence of adsorbed carboxylates.^{6,23}

CONCLUSIONS

To summarize, SXRD data have been acquired from an X-ray-induced superhydrophilic rutile- $TiO_2(110)(1 \times 1)$ surface. It is concluded that the five-fold-coordinated surface Ti atom is hydroxylated, as indicated by the presence of an atom, assumed to be O, at a distance of 1.90 ± 0.02 Å. There is also evidence of hydrogen-bonded H_2O molecules, which are located somewhat further from the substrate surface. The examination of the current structure, in tandem with previous work,^{14,20} suggests that the X-ray-induced superhydrophilicity of titania is likely to be a result of both the depletion of surface carbon and increased surface hydroxylation.

ASSOCIATED CONTENT

Supporting Information

The Supporting Information is available free of charge on the ACS Publications website at DOI: 10.1021/acs.jpcc.9b00245.

Atomic coordinates for optimum structure determined in this study (CIF)

Figure S1. Ball-and-stick model of optimized superhydrophilic $TiO_2(110)$ surface, showing all atoms displaced during fitting of SXRD data. Table S1. Optimized coordinates of atoms obtained from fitting of SXRD data acquired from superhydrophilic rutile- $TiO_2(110)$ (PDF)

AUTHOR INFORMATION

Corresponding Author

*Tel: +44 161 306 4824. Fax: +44 161 306 4865. E-mail: robert.lindsay@manchester.ac.uk.

ORCID

G. Cabailh: 0000-0002-8053-2132

G. Thornton: 0000-0002-1616-5606

R. Lindsay: 0000-0001-5050-669X

Notes

The authors declare no competing financial interest.

ACKNOWLEDGMENTS

We very much appreciate the highly constructive discussion with Tetsuroh Shirasawa as well as his allowing us access to relevant data. This study was funded by an ERC Advanced Grant ENERGYSURF (G.T.), EPSRC (UK) (EP/C541898/1), EU COST action CM1104, the Royal Society, M.E.C. (Spain) through project MAT2015-68760-C2-2-P, Severo Ochoa SEV-2015-0496 Grant, and project EFA194/16/TNSI funded by Interreg POCTEFA Program. J.P.W.T. acknowledges support from Diamond Light Source.

REFERENCES

- (1) Wang, R.; Hashimoto, K.; Fujishima, A.; Chikuni, M.; Kojima, E.; Kitamura, A.; Shimohigoshi, M.; Watanabe, T. Light-Induced Amphiphilic Surfaces. *Nature* **1997**, *388*, 431–432.
- (2) Isaifan, R. J.; Samara, A.; Suwaileh, W.; Johnson, D.; Yiming, W.; Abdallah, A. A.; Aïssa, B. Improved Self-Cleaning Properties of an Efficient and Easy to Scale up TiO_2 Thin Films Prepared by Adsorptive Self-Assembly. *Sci. Rep.* **2017**, *7*, 9466.
- (3) Takeuchi, M.; Sakamoto, K.; Martra, G.; Coluccia, S.; Anpo, M. Mechanism of Photoinduced Superhydrophilicity on the TiO_2 Photocatalyst Surface. *J. Phys. Chem. B* **2005**, *109*, 15422–15428.
- (4) Adachi, T.; Lathe, S. S.; Gosavi, S. W.; Roy, N.; Suzuki, N.; Ikari, H.; Kato, K.; Katsumata, K.; Nakata, K.; Furudate, M.; et al. Photocatalytic, Superhydrophilic, Self-Cleaning TiO_2 Coating on Cheap, Light-Weight, Flexible Polycarbonate Substrates. *Appl. Surf. Sci.* **2018**, *458*, 917–923.
- (5) Midtdal, K.; Jelle, B. P. Self-Cleaning Glazing Products: A State-of-the-Art Review and Future Research Pathways. *Sol. Energy Mater. Sol. Cells* **2013**, *109*, 126–141.
- (6) Zubkov, T.; Stahl, D.; Thompson, T.; Panayotov, D.; Diwald, O.; Yates, J. Ultraviolet Light-Induced Hydrophilicity Effect on $TiO_2(110)(1 \times 1)$. Dominant Role of the Photooxidation of Adsorbed Hydrocarbons Causing Wetting by Water Droplets. *J. Phys. Chem. B* **2005**, *109*, 15454–15462.
- (7) Arimitsu, N.; Nakajima, A.; Katsumata, K.; Shiota, T.; Watanabe, T.; Yoshida, N.; Kameshima, Y.; Okada, K. Photoinduced Surface Roughness Variation in Polycrystalline TiO_2 Thin Films under Different Atmospheres. *J. Photochem. Photobiol., A* **2007**, *190*, 53–57.
- (8) Katsumata, K.; Nakajima, A.; Shiota, T.; Yoshida, N.; Watanabe, T.; Kameshima, Y.; Okada, K. Photoinduced Surface Roughness Variation in Polycrystalline TiO_2 Thin Films. *J. Photochem. Photobiol., A* **2006**, *180*, 75–79.

(9) Sakai, N.; Fujishima, A.; Watanabe, T.; Hashimoto, K. Quantitative Evaluation of the Photoinduced Hydrophilic Conversion Properties of TiO₂ Thin Film Surfaces by the Reciprocal of Contact Angle. *J. Phys. Chem. B* **2003**, *107*, 1028–1035.

(10) Lee, F. K.; Andreatta, G.; Benattar, J.-J. Role of Water Adsorption in Photoinduced Superhydrophilicity on TiO₂ Thin Films. *Appl. Phys. Lett.* **2007**, *90*, 181928.

(11) Sakai, N.; Fujishima, A.; Watanabe, T.; Hashimoto, K. Enhancement of the Photoinduced Hydrophilic Conversion Rate of TiO₂ Film Electrode Surfaces by Anodic Polarization. *J. Phys. Chem. B* **2001**, *105*, 3023–3026.

(12) Wang, R.; Hashimoto, K.; Fujishima, A.; Chikuni, M.; Kojima, E.; Kitamura, A.; Shimohigoshi, M.; Watanabe, T. Photogeneration of Highly Amphiphilic TiO₂ Surfaces. *Adv. Mater.* **1998**, *10*, 135–138.

(13) Shirasawa, T.; Voegeli, W.; Arakawa, E.; Takahashi, T.; Matsushita, T. Structural Change of the Rutile–TiO₂(110) Surface During the Photoinduced Wettability Conversion. *J. Phys. Chem. C* **2016**, *120*, 29107–29115.

(14) Ahmed, M. H. M.; Lydiatt, F. P.; Chekulaev, D.; Wincott, P. L.; Vaughan, D. J.; Jang, J. H.; Baldelli, S.; Thomas, A. G.; Walters, W. S.; Lindsay, R. Wet Chemically Prepared Rutile TiO₂(110) and TiO₂(011): Substrate Preparation for Surface Studies under Non-UHV Conditions. *Surf. Sci.* **2014**, *630*, 41–45.

(15) Diebold, U. The Surface Science of Titanium Dioxide. *Surf. Sci. Rep.* **2003**, *48*, 53–229.

(16) Vlieg, E. A. (2 + 3)-Type Surface Diffractometer: Mergence of the z-Axis and (2 + 2)-Type Geometries. *J. Appl. Crystallogr.* **1998**, *31*, 198–203.

(17) Vlieg, E. ROD: A Program for Surface X-Ray Crystallography. *J. Appl. Crystallogr.* **2000**, *33*, 401–405.

(18) Ahmed, M. H. M.; Torrelles, X.; Treacy, J. P. W.; Hussain, H.; Nicklin, C.; Wincott, P. L.; Vaughan, D. J.; Thornton, G.; Lindsay, R. Geometry of α -Cr₂O₃(0001) as a Function of H₂O Partial Pressure. *J. Phys. Chem. C* **2015**, *119*, 21426–21433.

(19) Cabailh, G.; Torrelles, X.; Lindsay, R.; Bikondoa, O.; Joumard, I.; Zegenhagen, J.; Thornton, G. Geometric Structure of TiO₂(110)(1 × 1): Achieving Experimental Consensus. *Phys. Rev. B: Condens. Matter Mater. Phys.* **2007**, *75*, 241403.

(20) Hussain, H.; Tocci, G.; Woolcot, T.; Torrelles, X.; Pang, C. L.; Humphrey, D. S.; Yim, C. M.; Grinter, D. C.; Cabailh, G.; Bikondoa, O.; et al. Structure of a Model TiO₂ Photocatalytic Interface. *Nat. Mater.* **2017**, *16*, 461–466.

(21) Nadeem, I. M.; Treacy, J. P. W.; Selcuk, S.; Torrelles, X.; Hussain, H.; Wilson, A.; Grinter, D. C.; Cabailh, G.; Bikondoa, O.; Nicklin, C.; et al. Water Dissociates at the Aqueous Interface with Reduced Anatase TiO₂(101). *J. Phys. Chem. Lett.* **2018**, *9*, 3131–3136.

(22) Huš, M.; Urbic, T. Strength of Hydrogen Bonds of Water Depends on Local Environment. *J. Chem. Phys.* **2012**, *136*, 144305.

(23) Balajka, J.; Hines, M. A.; DeBenedetti, W. J. I.; Komora, M.; Pavelec, J.; Schmid, M.; Diebold, U. High-Affinity Adsorption Leads to Molecularly Ordered Interfaces on TiO₂ in Air and Solution. *Science* **2018**, *361*, 786–789.